EXPERIMENTAL STUDIES OF COHERENT LIGHT PROPAGATION UNDER MULTIPLE SCATTERING CONDITIONS

O.I. BARCHUK, A.A. GOLOBORODKO, V.N. KURASHOV

Taras Shevchenko Kyiv National University, Faculty of Radiophysics
(6, Academician Glushkov Ave., Kyiv 03022, Ukraine)

UDC 538.5

Light scattering in the model where a layered medium is presented by a certain number of interfaces has been studied. The characteristics of vector fields after their transmission through every interface between media with different refractive indices have been calculated numerically. The results of calculations are in good agreement with experimentally measured dependences.

1. Introduction

The system of the Maxwell equations allows one to adequately describe the generation and propagation of electromagnetic waves in a homogeneous medium with regular boundary conditions [1]. The transmission of electromagnetic waves through an interface between two media with different optical properties (the refractive indices, anisotropies, nonlinear properties) can be analyzed in the framework of Maxwell's formalism with regard for the relevant boundary conditions. If the roughnesses are distributed randomly over the interface, the problem becomes more complicated and requires to analyze the stochastic equation with random boundary conditions. The fractal theory of scattering allows one to avoid a plenty of boundary conditions in the case of one scattering event. The problems of this type have been repeatedly examined in the literature (see, e.g., works [2—7]). However, the problem acquires a qualitatively new character if the scattering is multiple and occurs in statistically inhomogeneous media, because the coefficients of the corresponding stochastic equations are random fields. As a rule, such equations have no analytical solutions, being rather difficult for numerical analysis as well. Therefore, the search for relatively simple models that would be adequate in a certain approximation to the process of wave propagation in a random medium with multiple scattering seems expedient.

One of such models is the phase screen approximation. This method is well-known when being applied in the scalar approximation of the diffraction problem [8], e.g., while studying the wave propagation in a turbulent atmosphere [9]. Nevertheless, provided certain confinements, it can also be suitable for the problem of multiple scattering, when the wave propagation is considered as the wave transmission through a sequence of phase screens with corresponding statistical properties. The choice of those or other phase relations is caused by the physical features of scattering mechanisms.

One of the possible mechanisms, which directly governs the wave propagation through a layered dielectric medium, consists in the consecutive refraction of the wave by every layer interface, with stochastic boundary conditions being taken into account. Taking advantage of the Fresnel diffraction allows one to avoid a plenty of boundary conditions, both in the case of the Maxwell equations and in the fractal theory, and to consider the peculiarities of the speckle structure formation without invoking the approximations of geometrical optics. In so doing, every interface is simulated by a set of elements on the plane which are spatially distributed according to a certain statistical law [10]. The relevant physical phenomena can be characterized by the corresponding Fresnel reflection and transmission coefficients for every element of the interface [11]. They provide insight into the vector

structure of the field created by this wave and, in particular, give information about the state of its polarization. Since the interface is a random field in the general case, the polarizations of the reflected and refracted waves vary chaotically in space, which can be regarded as the spatial depolarization of the field. But in the case of single scattering, the variations of the polarization degree are insignificant [11].

On the other hand, in the case of multiple scattering, one may expect for a substantial depolarization of the scattered wave [12, 13]. Therefore, it is the polarization dependences that are expedient to be used in the framework of the given model of a multilayered medium to analyze its structure and physical properties. First of all, we note that the vector structure of the scattered-wave field in the Fresnel diffraction approximation can be calculated by applying the procedure, which was described in work [13], consecutively at every interface. Indeed, it is a direct problem, and no questions arise about the existence and uniqueness of the solutions obtained. This work is aimed at determining the polarization characteristics of a wave scattered by the multilayered medium.

2. Basic Relations

Consider the basic principles, which the scattering model is based on. The geometry of scattering at every layer interface is similar to that described in work [11] and is presented in Fig. 1.

A Gaussian beam with wavelength λ illuminates a rough surface $z(x, y)$ at an angle of incidence φ_i. The determination of the polarization characteristics of the scattered-wave field will be carried out in terms of the coherence matrix which has the following form for the scattered wave in the laboratory coordinate system:

$$\mathbf{I} = \begin{pmatrix} \langle E_x(\mathbf{R})E_x^*(\mathbf{R})\rangle & \langle E_x(\mathbf{R})E_y^*(\mathbf{R})\rangle \\ \langle E_y(\mathbf{R})E_x^*(\mathbf{R})\rangle & \langle E_y(\mathbf{R})E_y^*(\mathbf{R})\rangle \end{pmatrix}. \quad (1)$$

Here, $\mathbf{E}$ is the vector of the electric field strength of the scattered beam, and the averaging of the vector components of the electric field strength is carried out over the whole aperture of the beam. In this case, the intensity distribution depends on the coordinate $\mathbf{R}$ and the aperture arrangement in the plane of observation [10]. The polarization degree P is defined in terms of elements of the coherence matrix $\mathbf{I}$ as

$$P = \sqrt{1 - \frac{4(I_{xx}I_{yy} - I_{xy}I_{yx})}{(I_{xx} + I_{yy})^2}}. \quad (2)$$

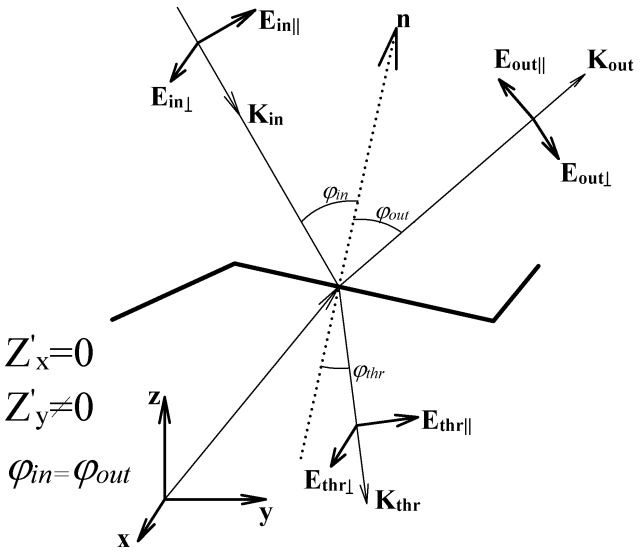

Fig. 1. Scattering geometry at a rough surface. Notations $\perp$ and $\parallel$ correspond to the local coordinate system which is connected to microplanes

In order to find the components of the correlation matrix, let us determine firstly the components of the wave vectors of the refracted and reflected waves. For this purpose, consider the refraction and reflection of light at an arbitrarily inclined plane surface of the medium with a given refractive index. The vector $\mathbf{n}$ normal to the surface can be presented as follows:

$$\mathbf{n} = \left(0; \frac{-Z_y'}{\sqrt{1+Z_y'^2}}; \frac{1}{\sqrt{1+Z_y'^2}}\right). \quad (3)$$

Then, the wave vector of the reflected wave in the laboratory coordinate system XYZ after obvious transformations looks like

$$\mathbf{K}^{\text{out}} = \begin{pmatrix} 0 \\ \frac{(1-Z_y'^2)k_{\text{in}Y} - 2k_{\text{in}Z}Z_y'}{1+Z_y'^2} \\ \frac{(1-Z_y'^2)k_{\text{in}Z} + 2k_{\text{in}Y}Z_y'}{1+Z_y'^2} \end{pmatrix}. \quad (4)$$

Here, $k_{\text{in}X}$ and $k_{\text{in}Y}$ are the wave vector components of the incident wave. In expression (3), the proper choice of the coordinate system allows one to take a certain symmetry of the model into account: since $Z_x' = 0$, all the coordinates $k_{\text{in}X} = 0$. Therefore, in this case, the nonzero reflection coefficients M can be presented in the form

$$M_{xx} = R_\perp, \quad M_{yy} = R_\parallel K_Z^{\text{out}}, \quad M_{zy} = R_\parallel K_Y^{\text{out}}, \quad (5)$$

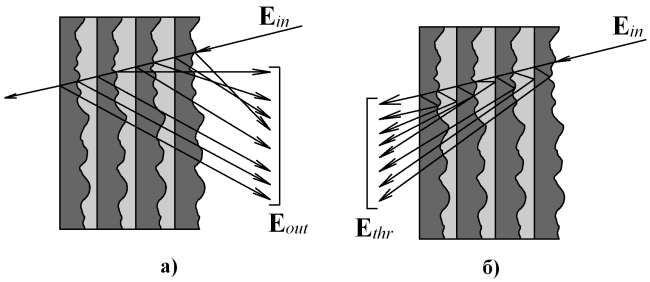

Fig. 2. Scenarios of wave scattering in multilayered structures: (a) a reflected wave and (b) a refracted wave

where $R_\perp$ and $R_\parallel$ are the local Fresnel coefficients for reflected waves. Correspondingly, the wave vector of the refracted wave in the laboratory coordinate system XYZ is

$$\mathbf{K}^{\rm thr} = \begin{pmatrix} 0 \\ \frac{k_{{\rm in}Z} Z'_y + k_{{\rm in}Y} - Z'_y \sqrt{n^2 - (k_{{\rm in}Z} Z'_y + k_{{\rm in}Y})^2}}{2n} \\ \frac{k_{{\rm in}Z} Z'^2_y + k_{{\rm in}Y} Z'_y - \sqrt{n^2 - (k_{{\rm in}Z} Z'_y + k_{{\rm in}Y})^2}}{2n} \end{pmatrix}, \quad (6)$$

where n is the index of refraction. Making use of expression (6), let us determine the transmission factors T. Among them, the following ones turn out to be nonzero:

$$T_{xx} = D_\perp, \quad T_{yy} = D_\parallel K_Y^{\rm out}, \quad T_{zy} = D_\parallel K_Z^{\rm out}. \quad (7)$$

Here, $D_\perp$ and $D_\parallel$ are the local Fresnel coefficients for refracted waves. Relations (4) and (6) make it possible to find the components of the field vectors for the reflected and refracted waves at the interface between media with different refractive indices.

Thus, we can propose the model scenarios of the scattering in a multilayered structure which are presented in (Fig. 2,a) for a back-scattered wave and (Fig. 2,b) for a refracted wave. The structure is assumed to be composed of many reflecting layers with different refractive indices and diffusive interfaces. The interface between two layers is defined by a variation of the refractive index. In the general case, both boundaries of a layer can be rough. But, in experiment, we used specimens with one smooth flat side for simplification. Let an optical wave fall on the surface of one layer of the structure with the refractive index n_1. Some portion of light, being reflected, quits the medium. The other portion, being refracted, penetrates into the next layer. The refracted wave falls on the next interface, where the process repeats. The figures schematically depicted the directions of propagation of the scattered waves.

In the model chosen, the refractive index for the i-th layer was selected in the form $\Delta n_i = (-1)^i \Delta n$, where $\Delta n = {\rm const}$ (the first layer is characterized by the refractive index with the subscript $i = 0$). The vectors of the waves reflected from the i-th interface, $\mathbf{E}_i^{\rm out}$, and refracted at it, $\mathbf{E}_i^{\rm thr}$, can be expressed in the following form:

$$\mathbf{E}_i^{\rm out} = \mathbf{M}_i \mathbf{E}_{i-1}^{\rm thr}; \quad \mathbf{E}_i^{\rm thr} = \mathbf{T}_i \mathbf{E}_{i-1}^{\rm thr}; \quad \mathbf{M}_i^2 + \mathbf{T}_i^2 = 1. \quad (8)$$

The total refracted wave is the sum of partial waves that passed through the multilayered structure. Accordingly, the total reflected wave is the sum of partial waves reflected from it:

$$\mathbf{E}^T(\mathbf{R}) = \sum_i \mathbf{E}_i^{\rm thr}(\mathbf{R}); \quad \mathbf{E}^O(\mathbf{R}) = \sum_i \mathbf{E}_i^{\rm out}(\mathbf{R}). \quad (9)$$

In the course of the computer simulation, we considered the scattering by every interface of the multilayered insulator, as well as multiply scattered partial waves. The contribution of such multiply scattered waves was taken into account, if their intensity exceeded a certain given threshold (in our calculations, this threshold was selected as 10^{-4} times the intensity of the wave that fell on the given interface of the multilayered structure). In the cases, where the back-reflected wave penetrated into previous layers and had an intensity higher than the error preset, the statistics of its fluctuations caused by the scattering in all intermediate layers was taken into consideration. Since the experimental data presented below were obtained for the far zone, where the distance to the zone of observation was much larger than the surface roughness characteristics, we exhibit the ultimate results for the components of the fields $\mathbf{E}^T$ (the refracted wave) and $\mathbf{E}^O$ (the reflected wave) in the Fraunhofer zone:

$$E_x^T = \frac{\exp(j\mathbf{KR})}{4\pi R} \int\int E_x^0 \prod T_{xx}^i e^{(-\frac{2\pi}{\lambda} j(\mathbf{kr}+\mathbf{kn}))} dS,$$

$$E_y^T = \frac{\exp(j\mathbf{KR})}{4\pi R} \int\int E_y^0 \prod T_{yy}^i e^{(-\frac{2\pi}{\lambda} j(\mathbf{kr}+\mathbf{kn}))} dS,$$

$$E_z^T = \frac{\exp(j\mathbf{KR})}{4\pi R} \int\int E_y^0 \prod T_{yz}^i e^{(-\frac{2\pi}{\lambda} j(\mathbf{kr}+\mathbf{kn}))} dS, \quad (10)$$

$$E_x^O = \sum \frac{\exp(j\mathbf{KR})}{4\pi R} \int\int E_x^i M_{xx}^i e^{(-\frac{2\pi}{\lambda} j(\mathbf{kr}+\mathbf{kn}))} dS,$$

$$E_y^O = \sum \frac{\exp(j\mathbf{KR})}{4\pi R} \int\int E_y^i M_{yy}^i e^{(-\frac{2\pi}{\lambda} j(\mathbf{kr}+\mathbf{kn}))} dS,$$

$$E_z^O = \sum \frac{\exp(j\mathbf{KR})}{4\pi R} \int\int E_y^i M_{yz}^i e^{(-\frac{2\pi}{\lambda} j(\mathbf{kr}+\mathbf{kn}))} dS. \quad (11)$$

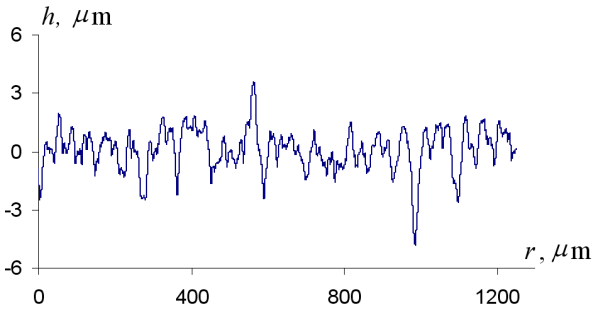

Fig. 3. Typical profile of a diffusion surface

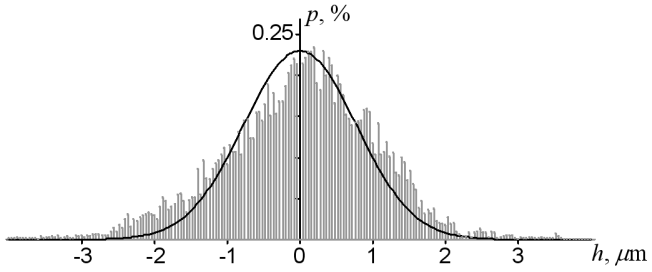

Fig. 4. Experimental and normal probability density functions for the surface height distribution

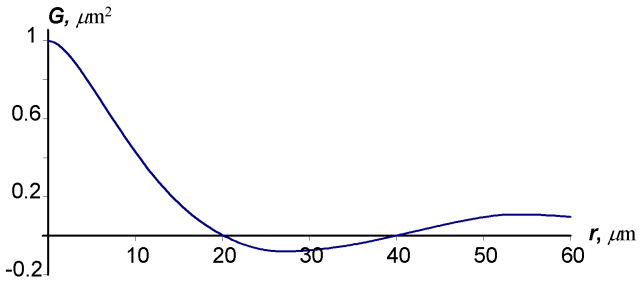

Fig. 5. Autocorrelation function for the diffusion surfaces with the parameters $\sigma = 1.1$ μm and $r = 11.4$ μm

Here, $\mathbf{r}$ is the coordinate in the reflecting surface plane, $\mathbf{R}$ an arbitrary coordinate in the plane of registration, $\mathbf{k}$ the wave vector, λ the wavelength, T^i and M^i are the local coefficients of refraction and reflection, respectively, at the interface between the i-th and $(i+1)$-th layers, E^i is the amplitude of the refracted wave at this interface, and $\mathbf{n}$ is the vector normal to the rough surface. The statistical averaging for each interface was carried out over independent samplings from the universal set of realizations of the random field of the relief. In such a way, using expressions (1), (2), (10), and (11), it is possible to find the polarization degree of the scattered waves, the magnitude of which is determined by the statistical characteristics of layer surfaces and their number.

3. Experimental Part

The experimental verification of the relations obtained was carried out for the model of a multilayered structure which consisted of a sequence of identical specimens made of milk glass with a random distribution of surface heights. An example of the surface profile is shown in Fig. 3.

All specimens were fabricated in a single technological run and had the identical dispersions of the height and correlation length distributions. In order to determine the height distribution of the surface profile, the sample function of the relevant probability density was plotted (see Fig. 4). Its shape corresponded rather well to that of the Gaussian-like distribution with a root-mean-square deviation $\sigma = 1.1$ μm.

Analogously, the independent measurements were fulfilled to obtain the autocorrelation function for the roughness profiles. The estimation of the autocorrelation function for the surface profile was carried out by the formula

$$G(l) = \frac{1}{K}\sum_{i=1}^{K-1} h_i h_{i-l}, \qquad (12)$$

where K is the number of discrete points of the profile along one line on the surface, and l is the distance between two points on the surface (the spatial shift). The average dispersion and correlation length were determined over 15 specimens. The number of experimentally measured points on every surface was $N = 40000$. The obtained autocorrelation function is shown in Fig. 5; its $\sigma = 1.1$ μm, and the correlation length at a level of $(1/e)$ was $r_K = 11.4$ μm. It was exactly these numerical values that were used to analyze experimental results.

The controllable conditions of the scattering were created by introducing the immersion liquids with various refractive indices between layers. In this case, the statistics of inhomogeneities was kept constant, and only one parameter — the dispersion of the optical path length in the interlayer interval — was varied, which was equivalent to the corresponding change of the profile height dispersion.

For the experimental determination of the coherence matrix components, the method of modulation polarimetry [14] was used. In the general case, the

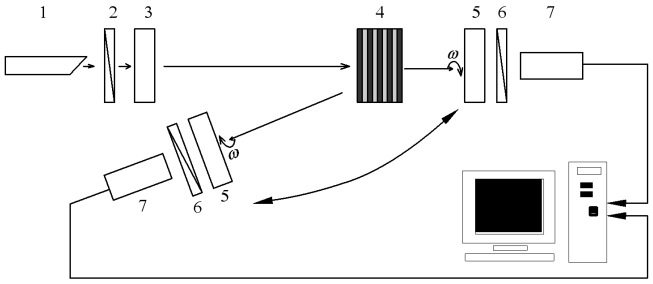

Fig. 6. Polarimeter scheme for measuring Müller matrices of the refracted and reflected radiation under multiple scattering conditions

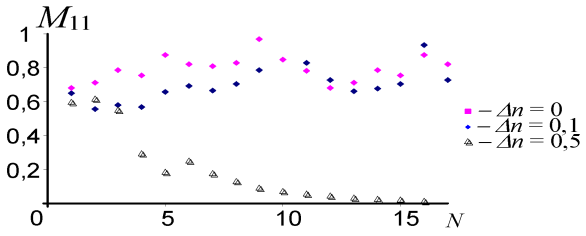

Fig. 7. Dependences of the first element of the Müller matrix M_{11} on the number of layers in the multilayered structure with various immersion liquids in the case of a refracted wave

method allows the elements of the Müller matrix to be measured and the complete information concerning the polarization structure of the radiation under study to be obtained. The scheme of a polarimeter used in experiment is shown in Fig. 6. By convention, it can be divided into two parts: the probing and reception channels. The medium to be studied is arranged between these components of the device. The probing channel, in its turn, consists of the following elements: a source of electromagnetic radiation with isotropic polarization *1*, a perfect polarizer *2*, and a quarter wavelength plate *3* with a computer-aided control of the azimuthal rotation angles. The reception channel is a device for measuring the Stokes vector components and includes a permanently rotating quarter wavelength plate *5*, a fixed analyzer *6*, and a photodetector *7*. The Fourier-transformation of the signal obtained gives the amplitudes of certain harmonics which are proportional to the Stokes vector components. The key parameters of the measuring system are described in work [15] in more details.

In the experiments, we used the emission radiation of a helium-neon laser with a wavelength of 0.63 μm. The laser beam, expanded up to 10 mm in diameter, illuminated a multilayered specimen, by falling normally to its surface. The measurement error was determined experimentally from the results of measurements of the Müller matrices for the standard optical elements [14,15]. The effective measurement error for the elements of the Müller matrix $\mathbf{M}$ was estimated by the relation

$$\delta M = \frac{\|M_{\text{exact}} - M_{\text{def}}\|}{\|M_{\text{exact}}\|}, \tag{13}$$

where M_{exact} and M_{def} are the exact and measured values, respectively, of the Müller matrix, and the notation $\|\ldots\|$ stands for the metric norm [15]. The magnitude of the error δM that was estimated in such a way did not exceed 1—1.5% [15].

4. Results and Their Discussion

In our experiments, we used optically isotropic media. Therefore, variations of the polarization state can be associated only with the distribution of surface inhomogeneities. In other words, the degree of light polarization at the output of the multilayered structure does not depend on the initial polarization state of the primary (probing) radiation. In the matrix representation, this means that the elements of the Müller matrix which govern a rotation of the polarization axis (phase optical elements) are zero [15]. In the general case of anisotropic objects, such a rotation of the polarization axes does exist.

The analysis of polarimetric measurements shows that the Müller matrix for an isotropic medium has the diagonal form

$$\mathbf{M}^{\text{thr}} = \begin{pmatrix} M_{11}^{\text{thr}} & 0 & 0 & 0 \\ 0 & M_{22}^{\text{thr}} & 0 & 0 \\ 0 & 0 & M_{33}^{\text{thr}} & 0 \\ 0 & 0 & 0 & M_{44}^{\text{thr}} \end{pmatrix}, \tag{14}$$

if light is transmitted through the medium (the elements with the superscript "thr"), or the form

$$\mathbf{M}^{\text{out}} = \begin{pmatrix} M_{11}^{\text{out}} & M_{12}^{\text{out}} & 0 & 0 \\ M_{21}^{\text{out}} & M_{22}^{\text{out}} & 0 & 0 \\ 0 & 0 & M_{33}^{\text{out}} & 0 \\ 0 & 0 & 0 & M_{44}^{\text{out}} \end{pmatrix}. \tag{15}$$

for media with back reflection (the elements with the superscript "out") [15].

Schematically, the measurement routine was organized as follows. Coherent linearly polarized laser emission illuminated a stack of milk glass plates with identical parameters of rough surfaces. The refractive index of glass, which the specimens were made of, was 1.495. To analyze how adequate the considered model is

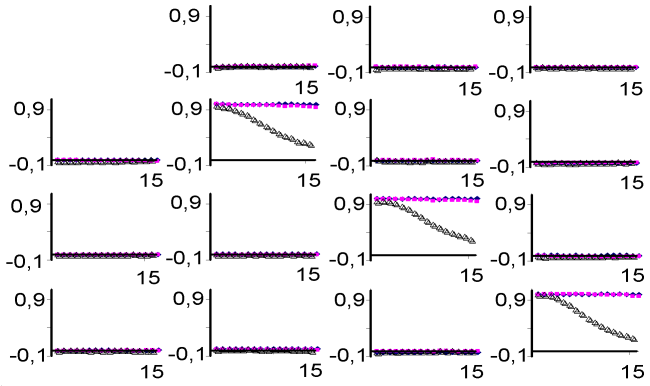

Fig. 8. Dependences of the normalized elements of the Müller matrix M_{ij} on the number of layers in the multilayered structure in the case of a refracted wave

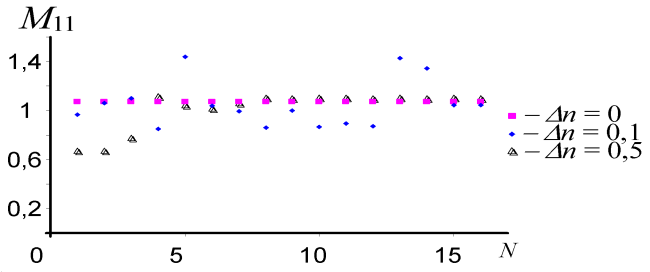

Fig. 9. The same as in Fig. 7, but for the reflected wave

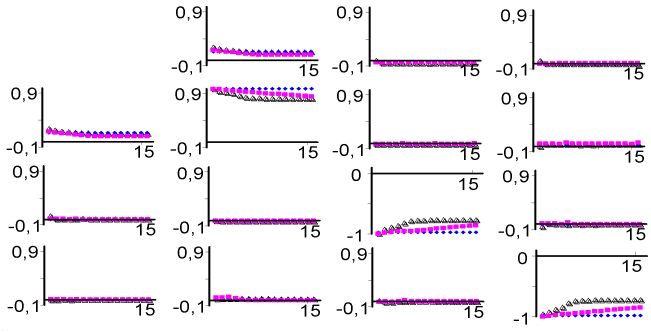

Fig. 10. The same as in Fig. 8, but for the reflected wave

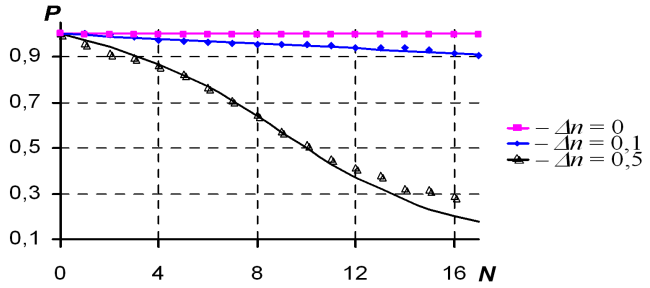

Fig. 11. Dependences of the polarization degree of the refracted wave on the number of layers in the multilayered structure with various immersion liquids

with respect to the real processes of coherent radiation depolarization by a multilayered medium with inhomogeneous interfaces, immersion liquids, as was said above, with the refractive indices of 1.38 and 1.501 were used. For the comparison of the obtained results with expressions (14) and (15) to be convenient, all the elements M_{ij} of the matrix **M** are depicted in Figs. 7 and 8. The first element of the Müller matrix M_{11} (Fig. 7) is the function, which the rest matrix elements are normalized by.

The reliability of all measurement results obtained for the matrix elements M_{ij} was checked by carrying out the corresponding complete and incomplete tests described in work [15]. In particular, the necessary conditions $M_{11} \geq 0$ and $M_{ij}/M_{11} \leq 1$ were verified, which can be considered as the incomplete testing. Generally speaking, the complete test corresponds to the analysis of all nonzero elements in the Müller matrix (the analysis for the emergence of anisotropy, nonlinear phenomena, and so on).

The elements of the Müller matrix for the back-reflected wave are shown in Figs. 9 and 10. Similarly to the previous case, the results for the first element of the Müller matrix M_{11} are shown in Fig. 9, while the normalized dependences for all the other elements (M_{ij}/M_{11}) in Fig. 10.

The main results of measurements of the polarization degree are shown in Figs. 11 and 12 for the cases of refracted and reflected waves, respectively. The solid curves correspond to the results of numerical calculations, provided that the parameters of the scattering surface are equal to the relevant values defined above. As one can see, the polarization degree of the scattered radiation depends not only on the total number of interfaces between layers with different refractive indices, but also on the refractive indices of the immersion liquids, i.e. on the equivalent roughness of the interface. In order to explain such dependences, one should bear in mind that the change of the radiation polarization at the interface between two layers with different refractive indices depends, according to the Fresnel formulas, on the difference between the refractive indices Δn. If, suppose, $\Delta n = 0$, the wave would remain completely polarized, because this case would simply mean the absence of the interface and, correspondingly, the absence of the scattering by

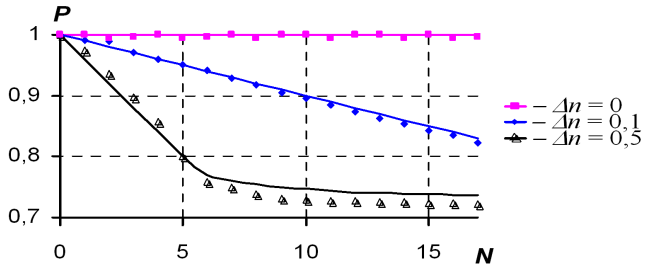

Fig. 12. The same as in Fig. 11, but for the reflected wave

the latter. Provided that $\Delta n \neq 0$, there occur some local variations of the polarization of the refracted and reflected waves, owing to the inclination of the wave vector with respect to the boundary segment plane. In this case, radiation becomes partially polarized because of the stochastically oriented segments. The increase of the layer number in the medium, as well as the increase of n, leads to the enhancement of this effect.

The difference between the dependences for the refracted (Fig. 11) and reflected (Fig. 12) waves is clearly observed. It can be explained by the availability of a polarized component due to the reflection of an almost completely polarized wave from several first interfaces, the specific number depending on the refractive index. The intensities of those components comprise a significant portion of the incident beam intensity. For example, the reflection coefficient for the first interface can be estimated, in supposition that $\Delta n \ll 1$, as

$$R^2 = \frac{\Delta n}{(n_i + n_{i+1})^2} = \frac{\Delta n}{(2n + \Delta n)^2} \approx \frac{\Delta n}{4n^2}. \qquad (16)$$

For the first plane, the reflection coefficient $R \approx 0.01$ at $\Delta n = 0.1$ and $R \approx 0.05$ at $\Delta n = 0.5$. Whence, it is clear that there will exist, at least, some final level of the polarization caused by the scattering at the first reflecting plane. As a result, the polarization degree of total radiation remains finite, even if the number of interfaces is arbitrary large. For any difference Δn between the refractive indices, there exists a definite threshold number of layers such that light can transmit them, but does not practically penetrate into the next layer. In this case, the polarization degree reaches some constant value and does not change any more further. Such a threshold number amounts to $N \approx 6 - 7$ at $\Delta n = 0.5$ (Fig. 12), while at $\Delta n = 0.1$ the threshold is reached at $N > 40$ (in experiment, this limit was not achieved).

5. Conclusions

Thus, a satisfactory agreement between the results of experimental measurements and those of computer simulations testifies to the adequacy of the model proposed to describe the scattering by a multilayered structure with inhomogeneous interfaces. However, such a description of the scattering processes has its limits of application, which are expedient to be indicated in more details. The validity of its application to the isotropic dielectric coatings with inhomogeneous layer interfaces is obvious. In a certain approximation, the model can also be suitable to analyze the propagation of polarized radiation in the dielectric wave guides with a step-like profile of the refractive index. At the same time, a similar model can be used as well to analyze the depolarization effects in anisotropic, randomly inhomogeneous media, where the resulting wave is formed by summing up separate partial waves and its stochastic polarization is induced by some physical mechanisms of anisotropy.

At last, we note one more a practically interesting feature of radiation depolarization in the framework of the considered model. Since the depolarization effects become considerably enhanced at the multiple scattering by rough interfaces, this enables the substantially more sensitive techniques of surface testing to be developed by introducing the optical feedback channel into the analyzing system, which ensures the wave to be reflected repeatedly from the surface under investigation. In this case, the quantitative characteristics of surface roughness may be determined by analyzing only the polarization contrast of the reflected wave, which considerably simplifies the construction of the corresponding polarimeter.

1. M. Born, E. Wolf, *Principles of Optics* (Pergamon Press, Oxford, 1980).
2. O.V. Angelsky, P.P. Maksimyak, Appl. Opt. **29**, 2894—2898 (1990).
3. T.A. Germer, C.C.Asmail, JOSA A, **16**, 1326—1332 (1999).
4. D.A. Zimnyakov, A.A. Mishin, A.N. Serov, Zh. Tekhn. Fiz. **67**, N 11, 101—112 (1997).
5. A.G. Ushenko, Opt. Eng. **34**, N4, 1088—1093 (1995).
6. S.N. Kulkov, Ya. Tomash, S.P. Buyakova, Pis'ma Zh. Tekhn. Fiz. **32**, N 2, 51—55 (2006).
7. E. Jakeman, J.Mc. Writer, P.N. Pusey, JOSA A **66**, №11, 1175—1182 (1976).
8. L.S. Andrews, R.L. Phillips, A.R. Weeks, Waves Random Media **7**, 229—244 (1997).
9. G.W. Goodman, *Statistical Optics* (John Wiley and Sons, New York, 1985).
10. V.N. Kurashov, V.V. Marienko, T.V. Molebna, A.G.Chumakov, Proc. SPIE **2647**, 48—56 (1995).

11. J.G. Fikioris, P.C. Waterman, J. Math. Phys. **5**, 1413—1420 (1969).

12. A.A. Goloborodko, V.N. Kurashov, Visn. Kyiv. Univ. N 2, 206—216 (2003).

13. R.N. Clark, T.L. Roush, J. Geophys. Res. **89**, 6329—6340 (1984).

14. S.N. Savenkov, Opt. Eng. **41**, 965—972 (2002).

15. M.I. Mishchenko, J.W. Hovenier, Opt. Lett. **20**, 1356—1358 (1995).

Received 28.02.06.
Translated from Ukrainian by O.I. Voitenko

ЕКСПЕРИМЕНТАЛЬНІ ДОСЛІДЖЕННЯ ПОШИРЕННЯ КОГЕРЕНТНОГО ВИПРОМІНЮВАННЯ ПРИ БАГАТОРАЗОВОМУ РОЗСІЯННІ

О.І. Барчук, А.О. Голобородько, В.Н. Курашов

Р е з ю м е

Використано модель розсіяння, в якій багатошарове середовище представлене набором певної кількості меж поділу. Чисельно розраховані характеристики векторних полів після проходження кожної межі для середовищ з різними показниками заломлення. Розрахунки було порівняно з експериментально виміряними залежностями, одержано хороше узгодження.